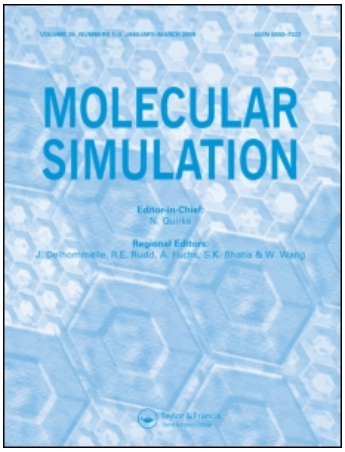

Molecular Simulation

Publication details, including instructions for authors and subscription information:
http://www.informaworld.com/smpp/title~content=t713644482

MD simulation of martensitic transformations in TiNi alloys with MEAM

H. Ishida[a]; Y. Hiwatari[b]
[a] Ishikawa National College of Technology, Ishikawa, Japan [b] Kanazawa University, Ishikawa, Japan

To cite this Article Ishida, H. and Hiwatari, Y.(2007) 'MD simulation of martensitic transformations in TiNi alloys with MEAM', Molecular Simulation, 33: 4, 459 — 461
To link to this Article: DOI: 10.1080/08927020701200942
URL: http://dx.doi.org/10.1080/08927020701200942

Molecular Simulation, Vol. 33, Nos. 4–5, 15–30 April 2007, 459–461

Taylor & Francis
Taylor & Francis Group

MD simulation of martensitic transformations in TiNi alloys with MEAM

H. ISHIDA†* and Y. HIWATARI‡¶

†Ishikawa National College of Technology, Tsubata, Ishikawa 929-0392, Japan
‡Kanazawa University, Kanazawa, Ishikawa 920-1192, Japan

(Received June 2006; in final form January 2007)

The martensitic transformations in TiNi alloys were studied using molecular dynamics (MD) simulations. The modified embedded atom method was used with the pseudo monoatomic potentials, which included angular dependence of each atoms. The thermally induced B2 → B19′ martensitic and B19′ → B2 reverse martensitic transformations have been obtained in the present molecular dynamics simulations with a bulk (no surface) computational model. The martensitic transformation temperature of TiNi varies very rapidly with composition in the range 35 ∼ 60 at.%Ni in the present MD simulations.

Keywords: Martensitic transformations; Molecular dynamics simulations; TiNi alloys; Modified embedded atom method

1. Introduction

The martensitic transformation is a first-order, displacive (displacements of atoms being much less than the atomic spacing) and diffusionless transition. In TiNi alloy, the high-temperature crystal structure called parent phase is B2 (ordered bcc structure), and the low-temperature crystal structure called martensitic phase is B19′ [1–5]. The martensitic transformation in TiNi alloy is a thermoelastic type transformation accompanied by a temperature hysteresis, a mobile twin interface and a crystallographically reversible transformation. The martensitic transformation temperature of TiNi varies very rapidly with composition in the range 40 ∼ 60 at.%Ni. The transformation temperature of $Ti_{0.5}Ni_{0.5}$ alloy is around the room temperature which is useful for the functionality materials.

The modified embedded atom method (MEAM) takes into account the screening effect of the interatomic interactions and angular dependence [6,7], while the embedded atom method (EAM) uses the electron density of a simple sum of radically dependent contributions from other atoms, less useful to the present study. The MEAM interactions can be very short ranged for atoms of a reasonably tight packed system, but can be long ranged for atoms in surface. The MEAM has been successfully used for the study of mechanical properties of the various crystal structures in alloy systems [8–12].

The purpose of the present work is to carry out MD simulations of the martensitic transformations in TiNi alloy with a bulk (no surface) computational model using the MEAM potentials so as to find these properties and construct a microscopic model for the martensitic transformations.

2. Simulation method

The martensitic transformation temperature of TiNi varies very rapidly with composition in the range 35–60 at.%Ni. We performed MD simulations with the MEAM potentials for the $Ti_{0.5}Ni_{0.5}$ alloy using the Gear algorithm, time step Δt ($= 1$ fs) and the 3-dimensional-periodic-boundary conditions.

The MEAM parameters; the sublimation energy E_i^0, the equilibrium nearest-neighbor distance r_i^0, the exponential decay factor for the universal energy function α_i, the scaling factor for the embedding energy A_i, the exponential decay factors for the atomic densities $\beta_i^{(l)}$ and the weighting factors for the atomic densities $t_i^{(l)}$ (modification of the $t_i^{(1)}$ value with Ref. [10]) for TiNi alloy are given in table 1. These parameters were

*Corresponding author. Tel.: + 81-76-288-8100. Fax: + 81-76-288-8102. Email: ishida@ishikawa-nct.ac.jp
¶Tel.: + 81-76-264-5674. Fax: + 81-76-264-5740. Email: hiwatari@cphys.s.kanazawa-u.ac.jp

Molecular Simulation
ISSN 0892-7022 print/ISSN 1029-0435 online © 2007 Taylor & Francis
http://www.tandf.co.uk/journals
DOI: 10.1080/08927020701200942

Table 1. The MEAM parameters for TiNi alloy; the sublimation energy E_i^0 (eV/atom), the equilibrium nearest-neighbor distance r_i^0 (Å), the exponential decay factor for the universal energy function α_i, the scaling factor for the embedding energy A_i, the exponential decay factors for the atomic densities $\beta_i^{(l)}$, the weighting factors for the atomic densities $t_i^{(l)}$, and the parameters of the smooth cut-off function $C_{\min}$, $C_{\max}$.

Atom	E_i^0	r_i^0	α_i	A_i	$\beta_i^{(0)}$	$\beta_i^{(1)}$	$\beta_i^{(2)}$	$\beta_i^{(3)}$	$t_i^{(1)}$	$t_i^{(2)}$	$t_i^{(3)}$	C_{min}	C_{max}
Ti	4.87	2.92	4.63	1.17	1.32	0	1.95	5	2.3	14.1	−5	2.0	2.8
Ni	4.450	2.49	4.99	1.10	2.45	2.2	6.0	2.2	5.79	1.60	3.70	2.0	2.8

determined from the experimental values: r_i^0, the atomic volume; α_i, the bulk modulus; A_i, the energy difference of structure; $\beta_i^{(0)}$, the shear elastic constant C_a; $\beta_i^{(1)}$, the internal relaxation for C_a; $\beta_i^{(2)}$, the shear elastic constants C_b and C_c; $\beta_i^{(3)}$, the shear elastic constant C_a; $t_i^{(1)}$, the vacancy formation energy; $t_i^{(2)}$, the shear elastic constants C_b and C_c; and $t_i^{(3)}$, the c/a ratio.

The Ni and Ti cross potential parameters; the sublimation energy $E_{\mathrm{TiNi}}^0 = (E_{\mathrm{Ti}}^0 + E_{\mathrm{Ni}}^0) - \Delta_{\mathrm{TiNi}}$, where $\Delta_{\mathrm{TiNi}} = -0.41\,\mathrm{eV/atm}$ is the enthalpy of formation the Ti and Ni atoms, the exponential decay factor for the universal energy function $\alpha_{\mathrm{TiNi}} = (\alpha_{\mathrm{Ti}} + \alpha_{\mathrm{Ni}})/2$, the equilibrium nearest-neighbor distance r_{TiNi}^0 calculated from the summed equilibrium intermetallic atomic volumes $\Omega_{\mathrm{TiNi}} = (\Omega_{\mathrm{Ti}} + \Omega_{\mathrm{Ni}})/2$. The enthalpy of formation for the TiNi in B19′; Δ_{TiNi} is calculated by the atomic sphere approximation linear Muffin-Tin orbital (ASA-LMTO) method [13].

The limiting value $C_{\min} = 2.80$ is assumed to be a little bit smaller than three so that the nearest neighbor atoms in the fcc structure ($C = 3$ for $r_{ik} : r_{ij} : r_{jk} = 1 : \sqrt{3}/2 : \sqrt{3}/2$) are unscreened in consideration of the thermal vibration. On the other hand, $C_{\min} = 2.0$ is the threshold value that the second neighbor atoms in the bcc structure ($C = 2$ for r_{ik}:r_{ij}:r_{jk} = 1:/2:/2) are just screened. Therefore, the influence of the thermal vibration on the second neighbor atoms in the bcc structure appears a little greatly for the phase transformation between B2 (ordered bcc structure) and B19′ in TiNi alloy. The $C_{\min}$ was altered into 2.35 from the original [8] value 2.0 to avoid this difficulty. By this change, the transformation temperature fell down and not only the transformation but also that reverse transformation have been obtained.

In the present MD simulation, the pressure of the system was controlled by the Parrinello–Rahman algorithm [14,15] with the external pressure $P_{\mathrm{ext}} = 0$ and the external stress $S_{\mathrm{ext}} = 0$. The temperature was controlled by the Nosé–Hoover thermostat [16,17]. MD simulations were started with a given initial structure and temperature with initial random velocities following the Boltzmann distribution.

The total number of atoms N is 432 for the present MD system of TiNi. The initial atom arrangement was set up from the condition of the B2 or B19′ structure configuration of $Ti_{0.5}Ni_{0.5}$ starting with a complete set of Ti or Ni atoms was substituted with some Ni or Ti atoms to obtain corresponding atomic compositions by using the random number. The equilibrium nearest-neighbor distance $r_{ij}^0 = \Omega^{1/3}$ is calculated from the summed equilibrium intermetallic atomic volumes Ω_{ij} for TiNi.

3. Results and discussions

3.1 Martensitic transformation by continuous cooling and heating processes

Starting with an initial state of B2 structure as a parent phase for Ti_xNi_{1-x} ($x = 0.5$) alloy, the temperature was first cooled down from $T = 1000$ to 100 K at the rate of 0.01 K/step, and then heated up to $T = 1000$ K at the same rate. The temperature dependence of three cell constants, h_{11}, h_{22} and h_{33} in this MD simulation is shown in figure 1. Three cell constants take similar values irrespective of both cooling and heating processes below 1000 K and above 100 K. Between 335 and 305 K they depend on either process, showing a hysteresis. In these simulations, the thermally induced B2–B19′ structural change and the reverse transformation were obtained. In order to examine those discrepancies between MD results and experiments further considerations are needed, such as size effects of the MD calculation, effects of the periodic boundary conditions used and so on.

3.2 Transformations structures

The thermally induced martensitic to B19′ transformations and the reverse transformations to B2 have been obtained in the present MD simulation for $Ti_xNi_{1-x}(x = 0.5)$ alloy as shown in figure 2.

A straining of the B2 structure along $[001]_{\mathrm{B2}}$, $[110]_{\mathrm{B2}}$ and $[1\bar{1}0]_{\mathrm{B2}}$ directions plus a $(110)[1\bar{1}0]_{\mathrm{B2}}$ shuffle produce the B19 orthorhombic structure. Then, a $(110)[1\bar{1}0]_{\mathrm{B2}}$, i.e. $(100)[00\bar{1}]_{\mathrm{B19}}$, homogeneous shear drives the B19 into the monoclinic B19′. The orientational relationship between the parent phase and martensitic phase of the atomic configuration, $(1\bar{1}0)_{\mathrm{B2}} \| (010)_{\mathrm{B19'}}$ and $[1\bar{1}0]_{\mathrm{B2}} \| [010]_{\mathrm{B19'}}$.

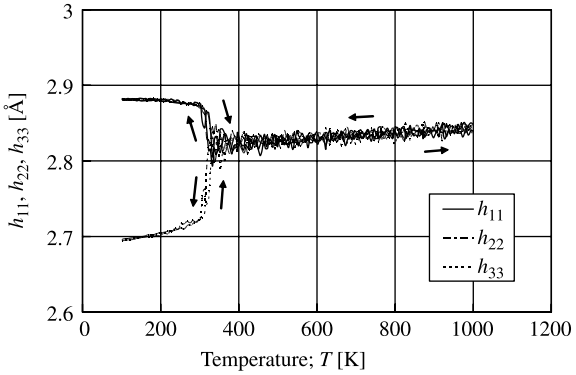

Figure 1. The temperature dependence of three cell constants for TiNi during the continuous cooling and heating process.

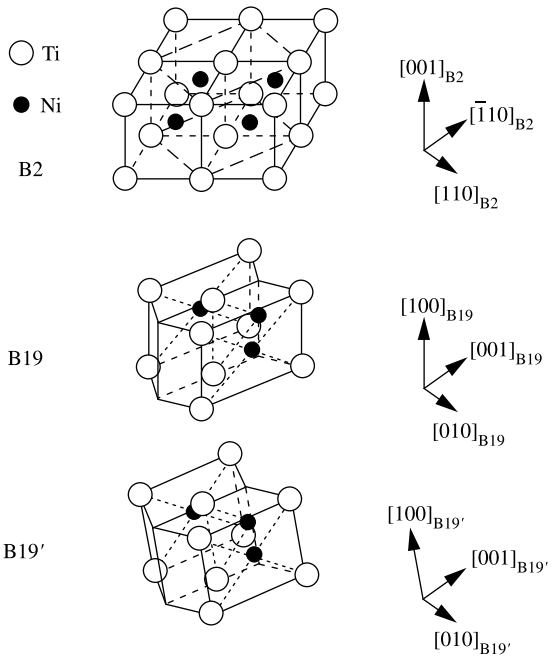

Figure 2. The schematic of the structural transformation from B2 to B19′ after Otsuka and Ren [18].

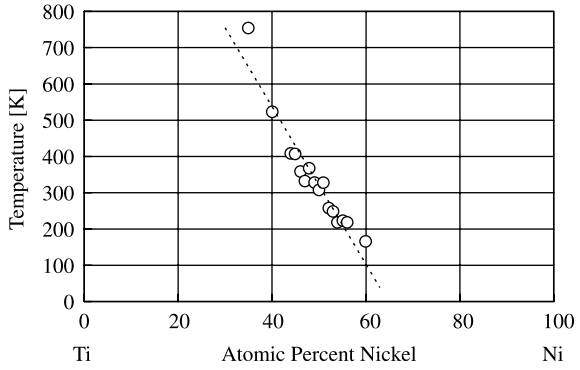

Figure 3. The concentration dependence of the transformation temperature *Ms* of TiNi. The broken line shows linear approximation.

3.3 Concentration dependence of the transformation temperature

The concentration dependence of the martensite-start temperature was studied by starting with an initial state of B2 structure as a parent phase for Ti_xNi_{1-x} ($0.35 < x < 0.6$) alloy, the temperature was cooled from $T = 1000$ to 100 K at the rate of 0.01 K/step. The concentration dependence of the transformation temperature is shown in figure 3. The sensitivity of the transformation temperature on composition 22 K/at.%Ni is lower than the experiments value [19], and the dependence of the transformation temperature for the concentration of Ti-rich TiNi alloy is not in agreement with experimental data.

4. Summary

The martensitic transformations in TiNi alloys were studied using MD simulations. The MEAM potential was used with the pseudo monoatomic potentials, which included angular dependence of each atoms. The thermally induced B2 → B19′ martensitic and B19′ → B2 reverse martensitic transformations have been obtained in the present molecular dynamics simulations with a bulk (no surface) computational model. The martensitic transformation temperature of TiNi varies very rapidly with composition in the range 35 ∼ 60at.%Ni in the present MD simulations.

References

[1] J.Y. Rhee, B.N. Harmon, D.W. Lynch. Optical properties and electronic structures of B2 and B19′ phases of equiatomic Ni–Ti alloys. *Phys. Rev. B*, **59**, 1878 (1999).
[2] M. Fukuhara, M. Yagi, A. Matsuo. Temperature dependence of elastic parameters and internal frictions for TiNi alloy. *Phys. Rev. B*, **65**, 224210 (2002).
[3] S.P. Gadaj, W.K. Nowacki, E.A. Pieczyska. Temperature evolution in deformed shape memory alloy. *Infrared Phys. Technol.*, **43**, 151 (2002).
[4] L.L. Meisner, V.P. Sivokha. The effect of applied stress on the shape memory behavior of TiNi-based alloys with different consequences of martensitic transformations. *Physica B*, **344**, 93 (2004).
[5] H. Rumpf, T. Walther, C. Zamponi, E. Quandt. High ultimate tensile stress in nano-grained superelastic NiTi thin films. *Mater. Sci. Eng. A*, **415**, 304 (2006).
[6] M.I. Baskes. Application of the embedded-atom method to covalent materials: a simiempirical potential for silicon. *Phys. Rev. Lett.*, **59**, 2666 (1987).
[7] M.I. Baskes, J.S. Nelson, A.F. Wright. Semiempirical modified embedded-atom potentials for silicon and germanium. *Phys. Rev. B*, **40**, 6085 (1989).
[8] M.I. Baskes. Modified embedded-atom potentials for cubic materials and impurities. *Phys. Rev. B*, **46**, 2727 (1992).
[9] M.I. Baskes, R.A. Jhonson. Modified embedded atom potentials for HCP metals. *Modelling Simul. Mater. Sci. Eng.*, **2**, 147 (1994).
[10] M.I. Baskes. Atomistic potentials for the molybdenum–silicon system. *Mater. Sci. Eng. A*, **261**, 165 (1999).
[11] M.I. Baskes. Determination of modified embedded atom method parameters for nickel. *Mater. Chem. Phys.*, **50**, 152 (1997).
[12] H. Ishida, S. Motoyama, K. Mae, Y. Hiwatari. Molecular dynamics simulation of martensitic transformations in NiAl alloy using the modified embedded atom method. *J. Phys. Soc. Jpn.*, **72**, 2539 (2003).
[13] A. Pasturel, C. Colinet, D. Nguyen Manh, A.T. Paxton, M. van Schilfgaarde. Electronic structure and phase stability study in the Ni–Ti system. *Phys. Rev. B*, **52**, 15176 (1995).
[14] M. Parrinello, A. Rahman. Crystal structure and pair potentials: a molecular-dynamics study. *Phys. Rev. Lett.*, **45**, 1196 (1980).
[15] M. Parrinello, A. Rahman. Polymorphic transitions in single crystals: a new molecular dynamics method. *J. Appl. Phys.*, **52**, 7182 (1981).
[16] S. Nosé. A unified formulation of the constant temperature molecular dynamics methods. *J. Chem. Phys.*, **81**, 511 (1984).
[17] W.G. Hoover. Canonical dynamics: Equilibrium phase-space distributions. *Phys. Rev. A*, **31**, 1695 (1985).
[18] K. Otsuka, X. Ren. Recent developments in the research of shape memory alloys. *Intermetallics*, **7**, 511 (1999).
[19] K. Otsuka, X. Ren. Physical metallurgy of Ti–Ni-based shape memory alloys. *Prog. Mater. Sci.*, **50**, 511 (2005).